Dynamics Simulation of Grasping Process of Underwater Vehicle-Manipulator System

Zong-Yu Chang
Ocean University of China
Yang Zhang (zhangyang@stu.ouc.edu.cn)
Ocean University of China https://orcid.org/0000-0001-7683-2266
Zhong-Qiang Zheng
Ocean University of China
Lin Zhao
Ocean University of China
Kun-Fan Shen
Ocean University of China

Original Article

Keywords: Underwater vehicle-manipulator system, Coupling dynamic, Grasping process, Vehicle control, Floating pase

Posted Date: December 22nd, 2020

DOI: https://doi.org/10.21203/rs.3.rs-132641/v1

Title page

Dynamics Simulation of Grasping Process of Underwater Vehicle-Manipulator System

Zong-Yu Chang, born in 1973, is currently a professor and a PhD supervisor at *College of Engineering*, *Ocean University of China, China.* His main research interests include theory of mechanism, underwater robotics, dynamics and control, ocean engineering.
Tel: +86-532-66781031; E-mail: zongyuchang@ouc.edu.cn

Yang Zhang, born in 1992, is currently a PhD candidate at *College of Engineering*, *Ocean University of China, China.* He received his master degree from *Ocean University of China, China*, in 2018. His research interests include underwater manipulator, dynamics and control.
E-mail: zhangyang@stu.ouc.edu.cn

Zhong-Qiang Zheng, born in 1986, is currently a lecturer at *College of Engineering, Ocean University of China, China.* He received his PhD degree on offshore engineering in *Ocean University of China, China*, in 2015. His research interests include robotics and ocean engineering.

Lin Zhao, born in 1964, is currently an associate professor at *Ocean University of China, China*. He received his master degree from *Tianjin Universtiy, China*, in 1987. His research interests include offshore engineering, marine hoses and ocean engineering.
Tel: +86-532-66781125; E-mail: zl_qingdao@163.com

Kun-Fan Shen, born in 1997, is currently a master candidate at *College of Engineering, Ocean University of China, China*.
E-mail: 1164258812@qq.com

Corresponding author：Zong-Yu Chang E-mail：zongyuchang@ouc.edu.cn
Yang Zhang E-mail：zhangyang@stu.ouc.edu.cn

ORIGINAL ARTICLE

Dynamics Simulation of Grasping Process of Underwater Vehicle-Manipulator System

Zong-Yu Chang[1, 2] • Yang Zhang[1, 2] • Zhong-Qiang Zheng[1] • Lin Zhao[1, 2] • Kun-Fan Shen[1]

Received xx xx, 2020;

Abstract: Underwater vehicle-manipulator system (UVMS) can be applied to fulfill different complex underwater tasks such as grasping, drilling, sampling, etc. It is widely used in the field of oceanographic research, marine exploration, military and commercial applications. In this paper, the dynamic simulation of UVMS is presented in the process of grasping an object. Firstly, the dynamic model of UVMS, which considers the change of the load of manipulator when the end effector of manipulator grasps the object, is developed. To compare different control conditions, the numerical simulation of grasping processes without/with vehicle attitude control are carried out. The results show that the coupling dynamics between the vehicle and the manipulator in the grasping process are clearly illustrated. The tracking position error of end effector without vehicle control is large and UVMS cannot complete the grasping task under this condition. Vehicle control can compensate the motion of vehicle due to the coupling effect caused by the motion of manipulator. This study will contribute to underwater operation mission for UVMS with floating base.

Keywords: Underwater vehicle-manipulator system • Coupling dynamic • Grasping process • Vehicle control • Floating base

1 Introduction

Underwater vehicle-manipulator system (UVMS) is a powerful tool for ocean exploration and marine environment observation [1]. It can also be applied to fulfill the different complex underwater operation tasks such as grasping, drilling, sampling, etc. Due to the unknown underwater environment caused by poor knowledge of the hydrodynamic coefficients, the floating base and under-actuated of the UVMS, strongly nonlinear and coupled dynamics and unpredictable external disturbances, these bring huge challenge for the underwater operation mission. Therefore motion coordination and disturbance compensation for UVMS need to be considered to reduce the coupling effect between the vehicle and the manipulator, [2-4].

Plenty of kinds of UVMS has been studied and developed in recent years. ALIVE robot (see Figure 1(a)) equipped with 2 hydraulic grasps for autonomous underwater docking and a 7 degree-of-freedoms (DOF) hydraulic manipulator used for valve turning task [5]. SAUVIM (see Figure 1(b)), a semi-autonomous UVMS equipped with an Ansaldo 7 DOF manipulator that developed in AMADEUS project [6], which was proposed for free floating underwater operation [7]. In RAUVI, TRIDENT and TRITON project, GIRONA 500 (see Figure 1(c)) is a lighter I-AUV of less than 200 kg, whose mass is lighter than ALIVE (3.5 ton) and SAUVIM (6 ton) [8]. Therefore, effects of the mass and geometry of vehicle and manipulator on dynamic coupling condition should be considered [9-10]. A lightweight multi-link symmetrical structure was carried out and designed to reduce the coupling effect on the vehicle caused by the motion of manipulator [11]. Meanwhile, dual arm UVMS was proposed and developed for cooperating manipulation in recent years [12]. Some UVMS with dual arms have been studied, such as DexROV (see Figure 1(d)) [13], Ocean One (see Figure 1(e)) [14], etc. Dual arms can balance the operation in both sides and improve the stability of UVMS.

✉ Zong-Yu Chang
zongyuchang@ouc.edu.cn

[1] College of Engineering, Ocean University of China, Qingdao 266100, China

[2] Key Lab of Ocean Engineering of Shandong Province, Qingdao 266100, China


(a) ALIVE [5]

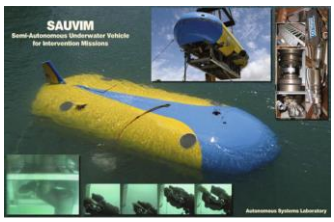

(b) SAUVIM [15]

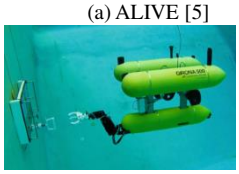
(c) GIRONA 500 [16]

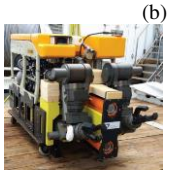
(d) DexROV [13]


(e) Ocean One [14]

Figure 1 Different kinds of UVMS

Underwater grasping is an important function for underwater operation. A UVMS requires coordinated motion and more robust and optimal control scheme to overcome some adverse factors. Sarkar and Podder [17] proposed a motion coordination planning strategy based on the optimized hydrodynamic drag force. Considering the redundancy of UVMS, Antonelli and Chiaverini [18] adopted a fuzzy task-priority inverse kinematics resolution approach to manage the vehicle-manipulator coordination. Han et al. [19] proposed a performance index for redundancy resolution of a UVMS, the restoring moments of the UVMS during manipulation could be reduced by optimizing the index. Considering manipulator joint limit, weighted minimum norm method can be applied in motion planning of UVMS [20]. Considering the collision avoidance, a local motion planning method for inspection mission had been presented and a trained artificial neural network was utilized [21]. According to sampling-based, search-based, and optimization-based motion planners, these algorithms and their performance with different metrics were analyzed and compared by qualitative/quantitative [22].

An indirect adaptive control method of UVMS for underwater manipulation tasks (pick and place operation) based on an extended Kalman filter was presented by Mohan and Kim, this method overcomes the disadvantages of direct adaptive control scheme and existing disturbance observers [23]. Then they carried out a coordinated motion control scheme using disturbance observer in task space [24]. Whereas a tracking controller with both joint-space and task-space tracking errors was proposed by Han, et al. [25]. Barbalata et al. [26] utilized force/motion controllers to handle a lightweight UVMS interaction with the underwater environment and compensate the coupling effects between the vehicle and the manipulator. Huang et al. [27] investigated the state of the art about dexterous operation underwater robot, underwater autonomous environmental perception, UVMS modeling and coordinated control, target grasping, etc. Acceleration-level task priority redundancy resolution method was proposed and remotely autonomous underwater with organism absorb or grasp function were analyzed and compared. Conti et al. [28] proposed a control architecture for intervention UVMS and studied on a suitable grasp planning strategy. Anderlini et al. [29] investigated an ROV with the consequent changes system dynamics when carried an object, an adaptive model predictive control scheme was proposed and its performance was compared with PID and sliding mode control. Many different control strategies for UVMS to track task trajectories were designed and carried out in recent years, such as adaptive backstepping control [30-31], model predictive control [32], sliding mode impedance control [33], and so on. Furthermore, vision based dexterous manipulation is also a useful form for underwater operations [34-36]. However, motion planning, advance control and sensing identification need higher technical support, these are hard to implement in practice. Therefore, a simple method is carried out in this paper by using PID control.

Considering dynamic coupling of the manipulator and the vehicle, interaction between the manipulator and the object, the changing of dynamic properties (such as mass and inertia of moment of end effector) when grasping an object, the dynamic simulation of grasping process of a floating underwater vehicle with a 3 DOF planar underwater manipulator is studied by using PID control scheme. This paper will be organized into five sections. Following the Introduction in section 1, the remainder of this paper is structured as follows. Section 2 introduces the dynamic modeling of UVMS, environment contacting force, actuator saturation, and modeling of end effector carrying an object. The PID controller is applied and the parameters of UVMS and controller are listed in section 3. In section 4, numerical simulation experiments are performed to verify without/with attitude control for vehicle. Finally, conclusions are made in section 5.

2 Dynamic Modeling of UVMS

According to the SNAME notation [37], the defined frames are as shown in Figure 2. $I(x, y, z)$ and $B(x_b, y_b, z_b)$ are earth-fixed (inertial) frame and vehicle body-fixed reference frame, respectively. $E(x_i, y_i, z_i)$ is the manipulator-end effector frame and $O(x_o, y_o, z_o)$ is the object reference frame.

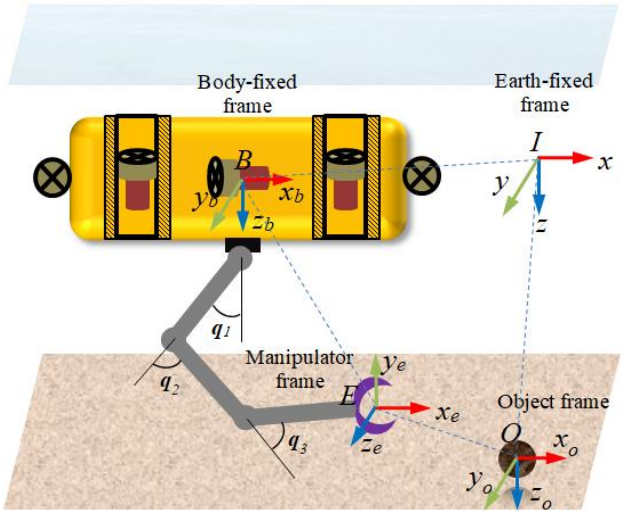

Figure 2 The model of UVMS equipped with a series manipulator and its coordinate frame

2.1 Kinematic of UVMS

The dynamics of an UVMS are highly coupled, strongly nonlinear and kinematic redundancy. Firstly, the vehicle general coordinates are defined in the earth-fixed frame.

$$\eta_v = \begin{bmatrix} \eta_1 \\ \eta_2 \end{bmatrix} = [\, x \quad y \quad z \quad \phi \quad \theta \quad \psi \,]^{\mathrm{T}}, \tag{1}$$

where $\eta_1 = [x\ y\ z]^{\mathrm{T}}$ represent motion displacement surge, sway and heave, respectively. $\eta_2 = [\phi\ \theta\ \psi]^{\mathrm{T}}$ represent Euler angles roll, pitch and yaw, respectively. Subscript v represents vehicle. The vector $\dot{\eta}_v$ is expressed the linear and angular velocities of the body of UVMS in the earth-fixed frame, which is the time derivative of the position and attitude η_v.

Considering the UVMS equipped with an n-DOF manipulator, $q_m = [q_1 \ \cdots \ q_n]^{\mathrm{T}} \in \mathbb{R}^{n\times 1}$ is the vector represents joints position (angle) of the corresponding underwater manipulator links, where n is the number of joints. Subscript m represents manipulator.

Then, define $\dot{\zeta} = [\mathbf{v}_v{}^{\mathrm{T}} \ \ \dot{q}_m{}^{\mathrm{T}}]^{\mathrm{T}} \in \mathbb{R}^{(6+n)\times 1}$ as the generalized velocity of the UVMS in the body-fixed frame. The linear and angular velocities of the origin of the body of UVMS in the body-fixed frame are define as

$$\mathbf{v}_v = \begin{bmatrix} v_v \\ \omega_v \end{bmatrix} \in \mathbb{R}^{6\times 1}, \tag{2}$$

where $v_v \in \mathbb{R}^{3\times 1}$ and $\omega_v \in \mathbb{R}^{3\times 1}$ denote the linear and angular velocity of the vehicle in the body-fixed frame.

Therefore, the generalized velocity in the earth-fixed frame can be obtained as follows:

$$\begin{bmatrix} \dot{\eta}_v \\ \dot{q}_m \end{bmatrix} = J(\eta_v)\dot{\zeta}, \tag{3}$$

The matrix $J(\eta_v) \in \mathbb{R}^{(6+n)\times(6+n)}$ is given by:

$$J(\eta_v) = \begin{bmatrix} R_B^I(\eta_2) & O_{3\times 3} & O_{3\times n} \\ O_{3\times 3} & J_o(\eta_2) & O_{3\times n} \\ O_{n\times 3} & O_{n\times 3} & I_{n\times n} \end{bmatrix}, \tag{4}$$

in which

$$R_B^I(\eta_2) = \begin{bmatrix} c\psi c\theta & c\psi s\phi s\theta - s\psi c\phi & s\psi s\phi + c\psi s\theta c\phi \\ s\psi c\theta & c\psi c\phi + s\psi s\theta s\phi & -c\psi s\phi + s\psi s\theta c\phi \\ -s\theta & c\theta s\phi & c\theta c\phi \end{bmatrix}$$

and

$$J_o(\eta_2) = \begin{bmatrix} 1 & t\theta s\phi & t\theta c\phi \\ 0 & c\phi & -s\phi \\ 0 & s\phi/c\theta & c\phi/c\theta \end{bmatrix}.$$

where $R_B^I \in \mathbb{R}^{3\times 3}$ is the linear velocity rotation matrix, $J_o \in \mathbb{R}^{3\times 3}$ is the angular velocity rotation matrix with $s\cdot = \sin(\cdot)$, $c\cdot = \cos(\cdot)$ and $t\cdot = \tan(\cdot)$. $I_{n\times n} \in \mathbb{R}^{n\times n}$ indicates the identity matrix and $O_{n_1\times n_2} \in \mathbb{R}^{n_1\times n_2}$ is the null matrix.

Let $\eta_{ee} = [\eta_{ee1} \ \ \eta_{ee2}]^{\mathrm{T}}$ denote the position and attitude vector of the end effector in the earth-fixed frame. $\eta_{ee1} \in \mathbb{R}^{3\times 1}$ and $\eta_{ee2} \in \mathbb{R}^{3\times 1}$ are the vector represents position and attitude of the end effector, respectively. The relationship between end effector velocity $\dot{\eta}_{ee}$ (expressed in the earth-fixed frame) and generalized velocity $\dot{\zeta}$ (the body-fixed system velocity expressed in the earth-fixed frame) can be obtained by:

$$\dot{\eta}_{ee} = J_k\left(R_B^I, q_m\right)\dot{\zeta}, \tag{5}$$

where $J_k\left(R_B^I, q_m\right) \in \mathbb{R}^{6\times(6+n)}$ is the Jacobian matrix of the UVMS.

2.2 Contact with Environment

If the end effector contacts with the environment (e.g., ground, wall, object, etc.), the force/moment at the tip of the manipulator acting on the whole UVMS can be expressed

$$\tau_e = J_k{}^{\mathrm{T}}\left(R_B^I, q_m\right)h_e, \tag{6}$$

where J_k is the Jacobain matrix defined in Eq. (5) and the vector $h_e \in \mathbb{R}^{6\times1}$ is defined as

$$h_e = \begin{bmatrix} f_e \\ t_e \end{bmatrix}, \tag{7}$$

in which f_e and t_e are the vector of forces and moments at the tip of the manipulator. Therefore, J_k is divided into two parts.

$$J_k\left(R_B^I, q_m\right) = \begin{bmatrix} J_{k,pos}\left(R_B^I, q_m\right) \\ J_{k,or}\left(R_B^I, q_m\right) \end{bmatrix} \in \mathbb{R}^{6\times(6+3)}, \tag{8}$$

We only consider the contact force at the end effector in this paper, and $J_{k,pos}\left(R_B^I, q_m\right) \in \mathbb{R}^{3\times(6+3)}$. Then combined with Eq. (6-8) and rewritten contact force equation

$$\tau_e = J_{k,pos}{}^{\mathrm{T}}\left(R_B^I, q_m\right) f_e, \tag{9}$$

in here, $f_e = K(\eta_{ee1} - \eta_o)$, $K > 0$ is the stillness matrix which has different value due to different environment and material, η_{ee1} and η_o are the position of the tip of end effector and the surface of the object.

2.3 Actuator Saturation

In fact, the actuator and motor control outputs are usually bounded by the thruster and motor physical limits.

$$\tau_{ci} = \begin{cases} \tau_{ci} & |\tau_{ci}| \le \tau_{ci,\max} \\ \tau_{ci,\max} & |\tau_{ci}| > \tau_{ci,\max} \end{cases}, \quad i = 1,\ldots,(6+n), \tag{10}$$

where $\tau_{ci,\max}$ is the actuator maximum control output limit for each DOF of UVMS. Desired input and actual output are shown in Figure 3.

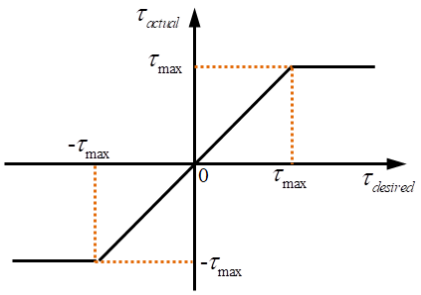

Figure 3 Desired input and actual output of actuator

Because of the thruster and motor's physical limits and constraints. The position, velocity, and acceleration of the UVMS are also bounded by the mechanical and physical limits.

$$\begin{cases} |\zeta_i| \le \zeta_{i,\max} \\ |\dot{\zeta}_i| \le \dot{\zeta}_{i,\max} \\ |\ddot{\zeta}_i| \le \ddot{\zeta}_{i,\max} \end{cases}, \quad i = 1,\ldots,(6+n), \tag{11}$$

where $\zeta_{i,\max}$, $\dot{\zeta}_{i,\max}$ and $\ddot{\zeta}_{i,\max}$ are the maximum allowed movement limit for each DOF of UVMS.

2.4 Modeling of End Effector Carrying an Object

When the end effector of UVMS carries an object, its dynamics are affected (see Figure 4). Hence, the model focuses on the scenario when the end effector has already grasped the body of object. Therefore, the object is assumed to be fixed in the end effector so that its position and attitude with respect of the end effector or end-link of the manipulator does not change. As a result, the end effector and the object can be modeled as a new rigid body, whose motions can be described by the same equations. However, the dynamic properties of end effector are changed in the process of grasping.

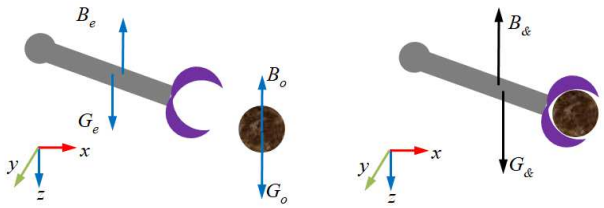

(a) Parted (b) Grabbed

Figure 4 The process of grasping an object of end effector

Before end effector grasps the object, the total mass of end effector or end-link of the manipulator is m_e, its volume V_e, the centers of buoyancy and gravity in the end effector body-fixed frame are ${}^b l_e^g$ and ${}^b l_e^b$, respectively. Then, the variables relating to the end effector are labeled as e, those relating to the object are labeled as o. And those corresponding to the combined body between end effector and object as &. $B = \rho g V$ and $G = mg$ are buoyancy and gravity of rigid body, respectively. in which ρ is seawater density and g gravitational acceleration. Hence the volume, mass and position of the centers of buoyancy

and gravity of the total end effector and object can be computed as follows:

$$V_{\&} = V_e + V_o, \tag{12}$$

$$m_{\&} = m_e + m_o, \tag{13}$$

$${}^{b}l_{\&}^{b} = \frac{V_e\,{}^{b}l_e^{b} + V_o\,{}^{b}l_o^{b}}{V_{\&}}, \tag{14}$$

$${}^{b}l_{\&}^{g} = \frac{m_e\,{}^{b}l_e^{g} + m_o\,{}^{b}l_o^{g}}{m_{\&}}, \tag{15}$$

By using the parallel axis theorem, the inertia matrix of changed end effector referenced to its body-fixed frame can obtained:

$$\begin{aligned} {}^{b}I_{\&,e} &= {}^{b}I_e - m_e S^2({}^{b}l_{\&}^{g} - {}^{b}l_e^{g}) \\ {}^{b}I_{\&,o} &= {}^{b}I_o - m_o S^2({}^{b}l_{\&}^{g} - {}^{b}l_o^{g}), \\ {}^{b}I_{\&} &= {}^{b}I_{\&,e} + {}^{b}I_{\&,o} \end{aligned} \tag{16}$$

where ${}^{b}I_e$ and ${}^{b}I_o$ are the inertia matrix of each body referenced to their center of gravity, and $S(\bullet) \in \mathbb{R}^{3\times3}$ is the skew symmetric matrix which is defined as follows.

$$S(x) = \begin{bmatrix} 0 & -x_3 & x_2 \\ x_3 & 0 & -x_1 \\ -x_2 & x_1 & 0 \end{bmatrix}, \tag{17}$$

2.5 Dynamic of UVMS

By using Newton-Euler equation, the dynamic equation of motion in the body-fixed frame of UVMS can be established as follows [38]:

$$M(\zeta)\ddot{\zeta} + C(\zeta,\dot{\zeta})\dot{\zeta} + D(\zeta,\dot{\zeta})\dot{\zeta} + G(\zeta) = \tau_e + \tau_c, \tag{18}$$

in which

$$M(\zeta) = \begin{bmatrix} M_v(\zeta_v) & H^{\mathrm{T}}(q_m) \\ H(q_m) & M_m(q_m) \end{bmatrix}$$

$$C(\zeta,\dot{\zeta}) = \begin{bmatrix} C_v(\zeta_v,\mathbf{v}_v) & 0 \\ 0 & C_m(q_m,\dot{q}_m) \end{bmatrix}$$

$$D(\zeta,\dot{\zeta}) = \begin{bmatrix} D_v(\zeta_v,\mathbf{v}_v) & 0 \\ 0 & D_m(q_m,\dot{q}_m) \end{bmatrix}$$

$$G(\zeta) = \begin{bmatrix} G_v(\zeta_v) \\ G_m(q_m) \end{bmatrix}, \tau_e = \begin{bmatrix} \tau_{ev} \\ \tau_{em} \end{bmatrix}, \tau_c = \begin{bmatrix} \tau_{cv} \\ \tau_{cm} \end{bmatrix}$$

where $M(\zeta) \in \mathbb{R}^{(6+n)\times(6+n)}$ is the mass matrix including added mass term, $C(\zeta,\dot{\zeta}) \in \mathbb{R}^{(6+n)\times(6+n)}$ represents the Coriolis and centripetal effects including added mass terms, $D(\zeta,\dot{\zeta}) \in \mathbb{R}^{(6+n)\times(6+n)}$ denotes the hydrodynamic force and damping matrix, $G(\zeta) \in \mathbb{R}^{(6+n)\times1}$ is the restoring matrix. $\tau_e \in \mathbb{R}^{(6+n)\times1}$ represents the external disturbances (such as end effector payloads, ocean currents, etc.) on the UVMS, $\tau_c \in \mathbb{R}^{(6+n)\times1}$ represents the controller input force/torques acting on the vehicle as well as joint. Comparing with single underwater robot and/or base-fixed manipulators, UVMS are more complex due to multi-body coupling and multi-body-fluid coupling effects.

3 Proportional-Integral-Derivative (PID) Control of UVMS

3.1 Proportional-Integral-Derivative (PID) control

In the process of UVMS grasping an object, the desired trajectory of end effector is planned in the inertial frame. The desired position η_{eed}, desired velocity $\dot{\eta}_{eed}$ and desired acceleration $\ddot{\eta}_{eed}$ of end effector are obtained by the quintic polynomial to generate fifth-order trajectories in task space. According to Eq. (3) and Eq. (5), the desired position, velocity and acceleration of the vehicle and manipulator joints in the body-fixed frame and earth-fixed frame can be obtained, respectively. The vector of position and velocity error of trajectory tracking can be expressed as:

$$\begin{bmatrix} \tilde{\eta}_v \\ \tilde{q}_m \end{bmatrix} = \begin{bmatrix} \eta_{vd} - \eta_v \\ q_{md} - q_m \end{bmatrix}, \tag{19}$$

$$\begin{bmatrix} \dot{\tilde{\eta}}_v \\ \dot{\tilde{q}}_m \end{bmatrix} = \begin{bmatrix} \dot{\eta}_{vd} - \dot{\eta}_v \\ \dot{q}_{md} - \dot{q}_m \end{bmatrix}, \tag{20}$$

The desired control force/torque acting on vehicle and manipulator joints in the inertial frame can be obtained as:

$$\begin{bmatrix} \tau_v \\ \tau_m \end{bmatrix} = \mathbf{K}_P \begin{bmatrix} \tilde{\eta}_v \\ \tilde{q}_m \end{bmatrix} + \mathbf{K}_I \int_0^t \begin{bmatrix} \tilde{\eta}_v(t') \\ \tilde{q}_m(t') \end{bmatrix} dt' + \mathbf{K}_D \begin{bmatrix} \dot{\tilde{\eta}}_v \\ \dot{\tilde{q}}_m \end{bmatrix}, \tag{21}$$

where $\mathbf{K}_P$, $\mathbf{K}_I$ and $\mathbf{K}_D$ are gain matrices and they are diagonal. τ_v and τ_m are desired control force/torque in inertial frame. Then the control scheme is converted to the body-fixed frame as

$$\tau_c = \begin{bmatrix} \tau_{cv} \\ \tau_{cm} \end{bmatrix} = J^{-1}(\eta_v) \begin{bmatrix} \tau_v \\ \tau_m \end{bmatrix}, \tag{22}$$

where τ_c is defined in Eq. (18) and its constraints are introduced in Eq. (10). The whole control schematic diagram is shown in Figure 5.

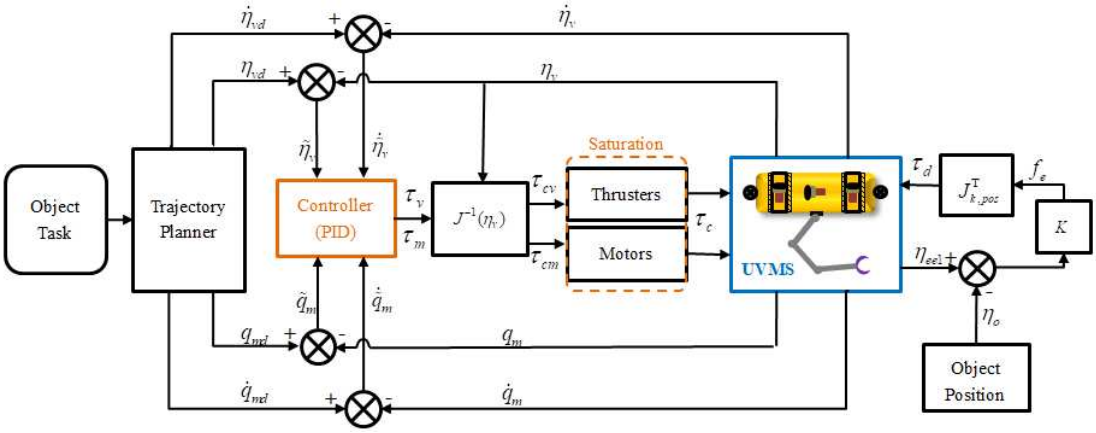

Figure 5 Schematic diagram of the UVMS control framework

3.2 Model Parameters

The parameters of UVMS in the following case study are referred to [39], the main parameters of vehicle and manipulator are listed in Table 1 and 2, respectively. The position of the base of manipulator is $[0, 0, 0.5]^T$ m in the vehicle body fixed frame, and the centers of mass and buoyancy of each links are $[0, 0, 0.5]^T$ m in their manipulator frame.

Table 1 Main parameters of the vehicle

Parameters		Value	Parameters		Value
Length [m]		5.3	Mass [kg]		5454.54
Buoyancy [N]		53400	Gravity [N]		53400
Center of buoyancy [m]		[0,0,0]	Center of mass [m]		[0,0,0.061]
Moment of inertia [kg•m^2]	I_{xx}	2038	Moment of inertia [kg•m^2]	I_{xy}	-13.58
	I_{yy}	13587		I_{yz}	-13.58
	I_{zz}	13587		I_{xz}	-13.58

Table 2 Main parameters of manipulator with 3-DOF links

Parameters		Link 1	Link 2	Link 3
Mass [kg]		31.4	20.1	15.4
q_m [rad]		q_1	q_2	q_3
Radius [m]		0.1	0.08	0.07
Length [m]		1	1	1
Viscous friction [Nms]		30	20	5
Moment of inertia [kg•m^2]	I_{xx}	1.65	0.75	0.4
	I_{yy}	11	6.3	4
	I_{zz}	11	6.3	4

Assuming that the object is modeled as a sphere, and its parameters are reported in Table 3. It is obvious that the weight of the object is greater than its buoyancy.

Table 3 Main parameters of the object

Parameters		Value	Parameters		Value
Sphere radius [m]		0.1	Mass [kg]		9.21
Buoyancy [N]		50.96	Gravity [N]		90.26
Moment of inertia [kg•m^2]	I_{xx}	0.037	Moment of inertia [kg•m^2]	I_{xy}	0
	I_{yy}	0.037		I_{yz}	0
	I_{zz}	0.037		I_{xz}	0

3.3 Controller Parameters

Assuming that the body of UVMS mounts thrusters can control vehicle translation and rotation (see Figure 2). For PID control, high gains can improve the controller response due to small trajectory tracking error. However, it will have different gains in different system. In this paper, the controller parameters that we choose for this UVMS simulation system are as follows:

$$\begin{aligned}
\mathbf{K}_P &= diag\{4000,\ 4000,\ 6000,\ 50000,\ 50000,\\
&\quad 50000,\ 4000,\ 1000,\ 500\}\\
\mathbf{K}_I &= diag\{0.2,\ 0.2,\ 0.5,\ 5,\ 3.55,\ 3,\ 2,\ 1,\ 0.5\},\\
\mathbf{K}_D &= diag\{8000,\ 8000,\ 20000,\ 50000,\ 65000,\\
&\quad 50000,\ 2000,\ 500,\ 200\}
\end{aligned} \tag{23}$$

4 Case Study

4.1 Simulation

The UVMS trajectory is planned with moving the end effector along a straight line in the absence of currents. Comparison simulation task is to pick up the object at start position $[0.5, 0, 2.5]^T$ m by the UVMS with the initial position and attitude of vehicle $[0, 0, 0, 0, 0, 0]^T$ m or deg

and the initial configuration of manipulator [-60, 90, 90]^T deg. And the goal position of the object is at [0, 0, 1.5]^T m. The whole process of manipulator for grasping and carrying the object is shown in Figure 6, and the time process is listed in Table 4.

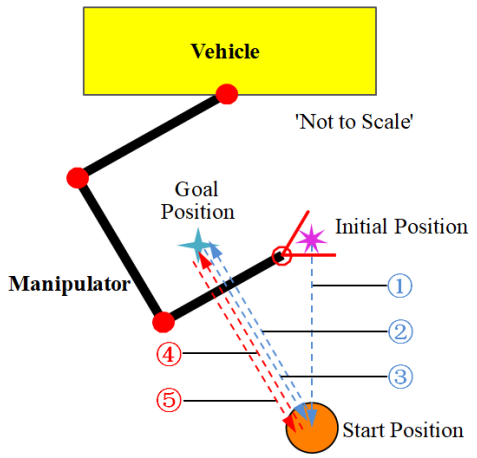

Figure 6 The process of grasping an object

Table 4 Time process of grasping operation

Number	Time [s]	Action of manipulator
①	0~25	From initial position to start position
②	25~40	From start position to goal position
③	40~55	From goal position to start position
-	55~60	Grasping operation
④	60~75	From start position to goal position
⑤	75~90	From goal position to start position

The desired motion of the vehicle is to keep stationary and only rotate manipulator joint. The desired position and attitude of vehicle η_{vd}, the desired velocity of vehicle $\dot{\eta}_{vd}$, the desired angle of manipulator joints q_{md} and the desired angular velocity of manipulator joints $\dot{q}_{md}$ are planned by trajectory planner using the quintic polynomial. The processes of grasping are simulated using MATLAB software. The total simulation time is 90 s and time step is 0.01 s.

The condition is considered firstly that the vehicle is floating and the thrusters cannot work to keep the vehicle position stationary while operation of manipulator. During the motion of the manipulator, the vehicle will move due to the coupling effect between the manipulator and the vehicle. Through numerical simulation, the actual distance between the tip of end effector and the position of start object position exceed 10 cm when pick up the object at t=55 s (Figure 7). Hence, the grasping task cannot be completed without vehicle control.

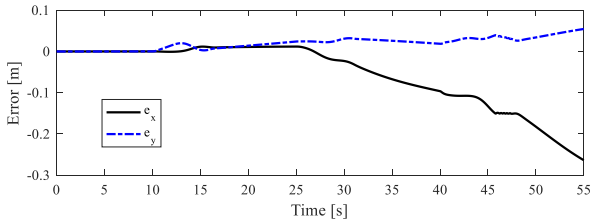

Figure 7 The position error of end effector without vehicle control

4.1.1 Case-I: Without attitude control for vehicle

The roll and pitch of the body of UVMS are able to hydrostatically stable because of the center of gravity of the vehicle is below the center of its buoyancy. When only the position of the vehicle is controlled, the whole UVMS system is under-actuated. In this situation, the desired control torque for control the attitude of the vehicle is set as 0. The desired and actual position of end effector response is shown in Figure 8, and the position trajectory tracking error of end effector is shown in Figure 9.

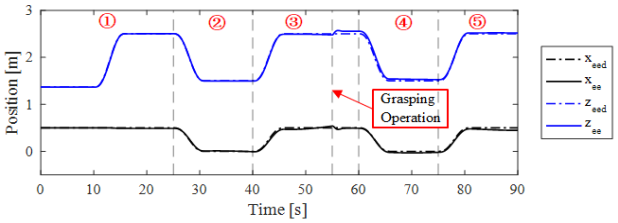

Figure 8 The desired and actual position of end effector with vehicle position control

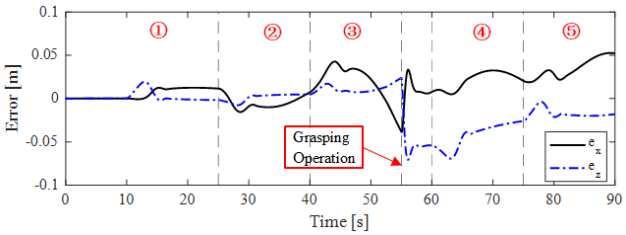

Figure 9 The position tracking error of end effector with vehicle position control

From Figure 8, when the manipulator picking up the object (at t=55 s), the distance between the tip of manipulator and the object is less than 10 cm. Although the vehicle attitude is not controlled, hydrostatically stable makes the vehicle Euler angle vary within a certain range below 2 deg (see Figure 13(c)). Hence, in this case the grasping task can be completed.

4.1.2 Case-II: With attitude control for vehicle

For a fully-actuated UVMS, the position and attitude of vehicle are controlled. Under this situation, the process of grasping operation is simulated. The desired and actual position of end effector response is shown in Figure 10, and the position trajectory tracking error of end effector is shown in Figure 11.

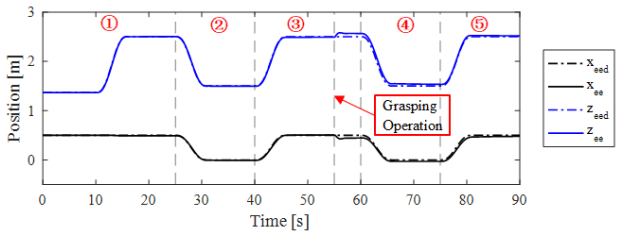

Figure 10 The desired and actual position of end effector with vehicle position and attitude control

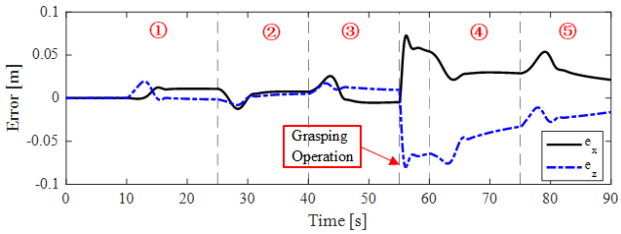

Figure 11 The position tracking error of end effector with vehicle position and attitude control

From Figure 10, when the manipulator picking up the object (at t=55 s), the distance between the tip of manipulator and the object is less than 1 cm. Under fully-controlled of vehicle, the position and attitude of vehicle vary over a small range. Hence, the grasping task in this situation can also be completed.

4.2 Results Comparison

Without the control for vehicle, the operation of manipulator cannot be completed for the coupling effect between the vehicle and the manipulator. Hence a comparative analysis of Case-I and Case-II is carried out. Due to the manipulator only moves in the vertical plane, the vehicle position y and vehicle Euler angle ϕ and ψ are always 0. So the trajectory of UVMS can be shown in Figure 12. The results show that PID control scheme is able to suit system dynamics changing and control UVMS carrying an object successfully.

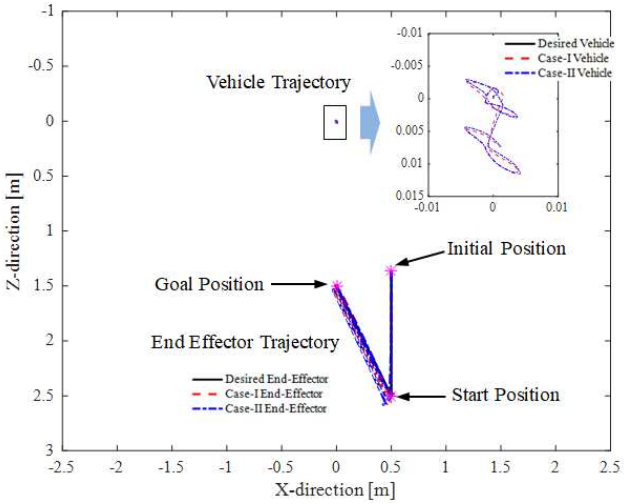

Figure 12 The trajectory of the position of the vehicle and the tip of end effector in vertical plane

The position of vehicle x and z, the Euler angle of vehicle θ, and manipulator joints q responses are shown in Figure 13. Their tracking errors are shown in Figure 14.

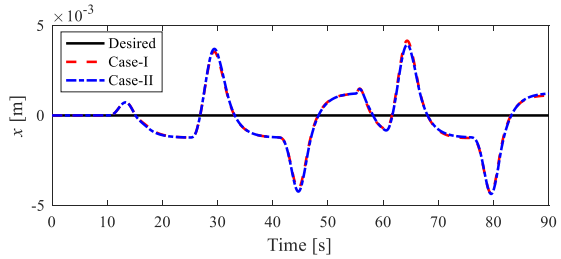

(a) Vehicle position response

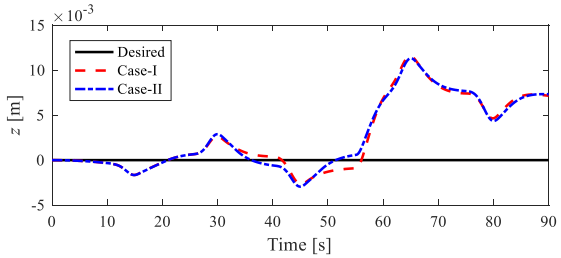

(b) Vehicle position response

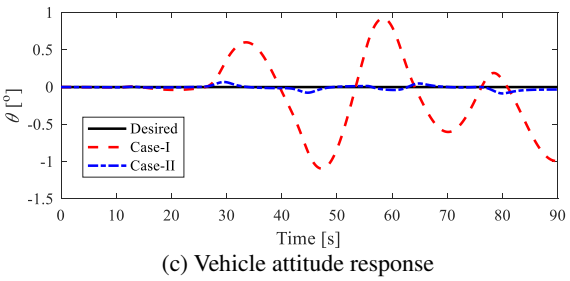

(c) Vehicle attitude response

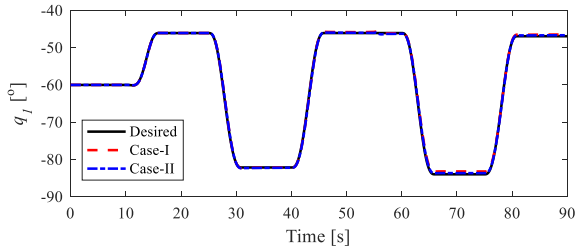

(d) Joint 1 trajectory responses

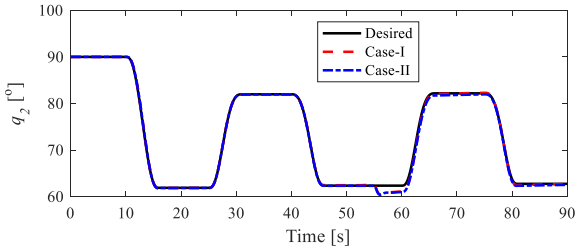

(e) Joint 2 trajectory responses

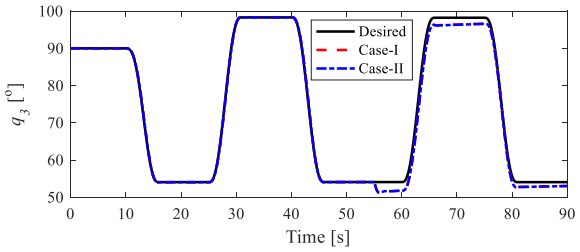

(f) Joint 3 trajectory responses

Figure 13 Vehicle and manipulator response

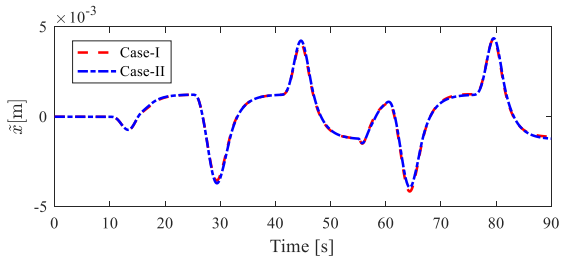

(a) Vehicle position error response

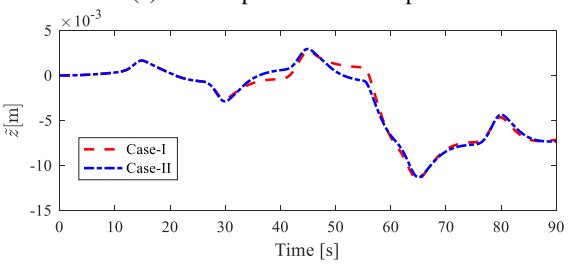

(b) Vehicle position error response

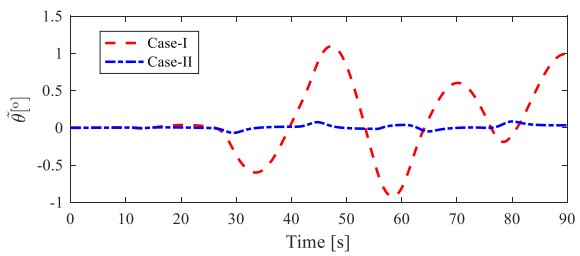

(c) Vehicle attitude error response

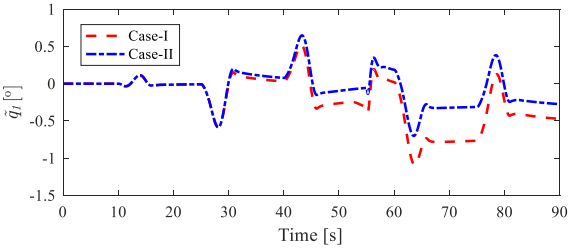

(d) Joint 1 error responses

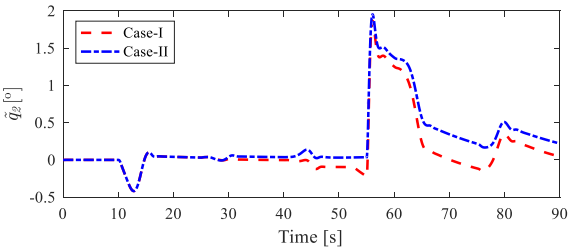

(e) Joint 2 error responses

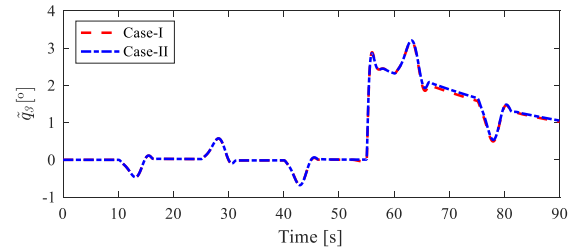

(f) Joint 3 error responses

Figure 14 Vehicle and manipulator errors response

From Figure 13 and 14, the pitch of vehicle with fully-controlled is less than only control for position. Moreover, the trajectories tracking errors are close in two cases except the attitude error of vehicle.

According to the root mean square error (RMSE) between actual and desired trajectories over the whole simulation duration for the 2 types of analyzed situation, the values of RMSE of the position and attitude of vehicle (V-X, V-Z, V-θ), manipulator joint angles (q_1, q_2, q_3), and the position of end effector (EE-X, EE-Z) are shown in Figure 15.

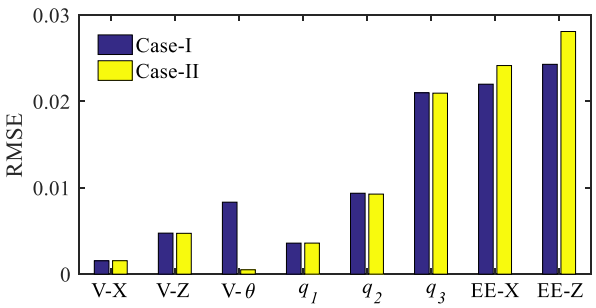

Figure 15 The RMSE of vehicle, manipulator and end effector

Due to vehicle attitude control, the values of RMSE of vehicle attitude are different in two cases. It is obvious that with vehicle attitude control can reduce attitude trajectory tracking error effectively. However, there is an interesting thing that the values of RMSE of end effector with vehicle attitude control are greater than without attitude control. This phenomenon shows that it may be because of the fixed PID parameters and the hydrostatic restoring force/moment of the vehicle. On the one hand, the system parameters of UVMS are changed, but PID parameters are fixed. On the other hand, the input attitude control force/moment and hydrostatic restoring force/moment affect each other, and this effect reduces the positioning accuracy of the end effector.

5 Conclusions

Dynamic simulation of the process of UVMS grasping an object is carried out and two cases that without/with vehicle attitude control are analyzed and compared in this article. Some conclusions are summarized as follows.

(1) A whole dynamic model of UVMS including actuator saturation, contact with environment, the changing of dynamic properties is derived. It contributes to handle the change of load of the manipulator and floating underwater operation.

(2) Two cases that without/with attitude control for vehicle are simulated and compared, it is obvious that the movement of manipulator can affect the position and attitude of the vehicle with floating base.

(3) The hydrostatic restoring force/moment is helpful for the stability of the UVMS system. However, the combined effect both hydrostatic restoring force/moment and system control force will affect the precise positioning of the end effector.

6 Declaration

Acknowledgements
Not applicable

Funding
Supported by National Natural Science Foundation of China (Grant No. 51875540)

Availability of data and materials
The datasets supporting the conclusions of this article are available from the corresponding author on reasonable request.

Authors' contributions
The author' contributions are as follows: Zong-Yu Chang was in charge of the whole trial; Yang Zhang and Zong-Yu Chang wrote the manuscript; Yang Zhang, Zhong-Qiang Zheng, Lin Zhao and Kun-Fan Shen assisted with sampling and laboratory analyses.

Competing interests
The authors declare no competing financial interests.

Consent for publication
Not applicable

Ethics approval and consent to participate
Not applicable

References

[1] M Lin, C Yang. Ocean observation technologies: A review. *Chinese Journal of Mechanical Engineering*, 2020, 33 (2): 33-50.

[2] M W Dunnigan, G T Russell. Evaluation and reduction of the dynamic coupling between a manipulator and an underwater vehicle. *IEEE Journal of Oceanic Engineering*, 1998, 23 (3): 260-273.

[3] T W McLain, S M Rock, M J Lee. Experiments in the coordinated control of an underwater arm/vehicle system. *Autonomous Robots*, 1996, 3 (2): 213-232.

[4] H Huang, G C Zhang, J Y Li, et al. Model based adaptive control and disturbance compensation for underwater vehicles. *Chinese Journal of Mechanical Engineering*, 2018, 31 (1): 114-126.

[5] J Evans, P Redmond, C Plakas, et al. Autonomous docking for intervention-AUVs using sonar and video-based real-time 3D pose estimation. *Proceedings of the MTS/IEEE Oceans 2003*, San Diego, CA, USA, 2003: 2201-2210.

[6] D M Lane, J B C Davies, G Robinson, et al. The AMADEUS dextrous subsea hand: Design, modeling, and sensor processing. *IEEE Journal of Oceanic Engineering*, 1999, 24 (1): 96-111.

[7] G Marani, S K Choi, J Yuh. Underwater autonomous manipulation for intervention missions AUVs. *Ocean Engineering*, 2009, 36 (1): 15-23.

[8] D Ribas, P Ridao, A Turetta, et al. I-AUV mechatronics integration for the TRIDENT FP7 project. *IEEE/ASME Transactions on Mechatronics*, 2015, 20 (5): 2583-2592.

[9] S Sivčev, J Coleman, E Omerdić, et al. Underwater manipulators: A review. *Ocean Engineering*, 2018, 163: 431-450.

[10] H Huang, Z Zhou, J Li, et al. Investigation on the mechanical design and manipulation hydrodynamics for a small sized, single body and streamlined I-AUV. *Ocean Engineering*, 2019, 186: 106106.

[11] C Tang, Y Wang, S Wang, et al. Floating autonomous manipulation of the underwater biomimetic vehicle-manipulator system: Methodology and verification. *IEEE Transactions on Industrial Electronics*, 2018, 65 (6): 4861-4870.

[12] H Farivarnejad, S A A Moosavian. Multiple impedance control for object manipulation by a dual arm underwater vehicle–manipulator system. *Ocean Engineering*, 2014, 89: 82–98.

[13] A Birk, T Doernbach, C A Müller, et al. Dexterous underwater

manipulation from onshore locations: Streamlining efficiencies for remotely operated underwater vehicles. *IEEE Robotics and Automation Magazine*, 2018, 25 (4): 24-33.

[14] O Khatib, X Yeh, G Brantner, et al. Ocean one: A robotic avatar for oceanic discovery. *IEEE Robotics and Automation Magazine*, 2016, 23 (4): 20-29.

[15] G Marani, J Yuh. *Introduction to autonomous manipulation: Case study with an underwater robot, SAUVIM*. New York: Springer-Verlag Berlin Heidelberg, 2014.

[16] D Ribas, N Palomeras, P Ridao, et al. Girona 500 AUV: From survey to intervention. *IEEE/ASME Transactions on Mechatronics*, 2012, 17 (1): 46-53.

[17] N Sarkar, T K Podder. Coordinated motion planning and control of autonomous underwater vehicle-manipulator systems subject to drag optimization. *IEEE Journal of Oceanic Engineering*, 2001, 26 (2): 228-239.

[18] G Antonelli, S Chiaverini. Fuzzy redundancy resolution and motion coordination for underwater vehicle-manipulator systems. *IEEE Transactions on Fuzzy Systems*, 2003, 11 (1): 109-120.

[19] J Han, J Park, W K Chung. Robust coordinated motion control of an underwater vehicle-manipulator system with minimizing restoring moments. *Ocean Engineering*, 2011, 38 (10): 1197-1206.

[20] M J Zhang, S Q Peng, Z Z Chu, et al. Motion planning of underwater vehicle-manipulator system with joint limit. *Applied Mechanics and Materials*, 2012, 220-223: 1767-1771.

[21] P Sotiropoulos, V Kolonias, N Aspragathos, et al. Rapid motion planning algorithm for optimal UVMS interventions in semi-structured environments using GPUs. *Robotics and Autonomous Systems*, 2015, 74: 15-29.

[22] D Youakim, P Ridao. Motion planning survey for autonomous mobile manipulators underwater manipulator case study. *Robotics and Autonomous Systems*, 2018, 107: 20-44.

[23] S Mohan, J Kim. Indirect adaptive control of an autonomous underwater vehicle-manipulator system for underwater manipulation tasks. *Ocean Engineering*, 2012, 54 (4): 233-243.

[24] S Mohan, J Kim. Coordinated motion control in task space of an autonomous underwater vehicle–manipulator system. *Ocean Engineering*, 2015, 104 (262): 155-167.

[25] H Han, Y Wei, X Ye, et al. Motion planning and coordinated control of underwater vehicle-manipulator systems with inertial delay control and fuzzy compensator. *Applied Sciences*, 2020, 10 (11): 3944.

[26] C Barbalata, M Dunnigan, Y Petillot. Coupled and decoupled force/motion controllers for an underwater vehicle-manipulator system. *Journal of Marine Science and Engineering*, 2018, 6 (3): 96.

[27] H Huang, Q Tang, J Li, et al. A review on underwater autonomous environmental perception and target grasp, the challenge of robotic organism capture. *Ocean Engineering*, 2020, 195: 106644.

[28] R Conti, F Fanelli, E Meli, et al. A free floating manipulation strategy for autonomous underwater vehicles. *Robotics and Autonomous Systems*, 2017, 87: 133-146.

[29] E Anderlini, G G Parker, G Thomas. Control of a ROV carrying an object. *Ocean Engineering*, 2018, 165: 307–318.

[30] J Wang, J Y Hung. Adaptive backstepping control for an underwater vehicle manipulator system using fuzzy logic. *Proceedings of the IECON 2018-44th Annual Conference of the IEEE Industrial Electronics Society*, Washington, DC, 2018: 5600-5606.

[31] C Yang, F Yao, M Zhang. Adaptive backstepping terminal sliding mode control method based on recurrent neural networks for autonomous underwater vehicle. *Chinese Journal of Mechanical Engineering*, 2018, 31 (1): 110.

[32] Y Dai, S Yu, Y Yan. An adaptive EKF-FMPC for the trajectory tracking of UVMS. *IEEE Journal of Oceanic Engineering*, 2019, 45 (3): 699-713.

[33] P Dai, W Lu, K Le, et al. Sliding mode impedance control for contact intervention of an I-AUV: Simulation and experimental validation. *Ocean Engineering*, 2020, 196: 106855.

[34] G Casalino, M Caccia, S Caselli, et al. Underwater intervention robotics: An outline of the Italian national project Maris. *Marine Technology Society Journal*, 2016, 50 (4): 98-107.

[35] Y Taira, S Sagara, M Oya. Model-based motion control for underwater vehicle-manipulator systems with one of the three types of servo subsystems. *Artificial Life and Robotics*, 2019, 25 (1): 133-148.

[36] J Li, H Huang, Y Xu, et al. Uncalibrated visual servoing for underwater vehicle manipulator systems with an eye in hand configuration camera. *Sensors*, 2019, 19 (24): 5469-5490.

[37] T I Fossen. *Handbook of marine craft hydrodynamics and motion control*. Chichester, West Sussex, UK: Wiley & Sons, 2011.

[38] G Antonelli. *Underwater robots*. 4th ed. Gewerbestrasse: Springer International Publishing AG, 2018.

[39] A J Healey, D Lienard. Multivariable sliding mode control for autonomous diving and steering of unmanned underwater vehicles. *IEEE Journal of Oceanic Engineering*, 1993, 18 (3): 327-339.

Figures

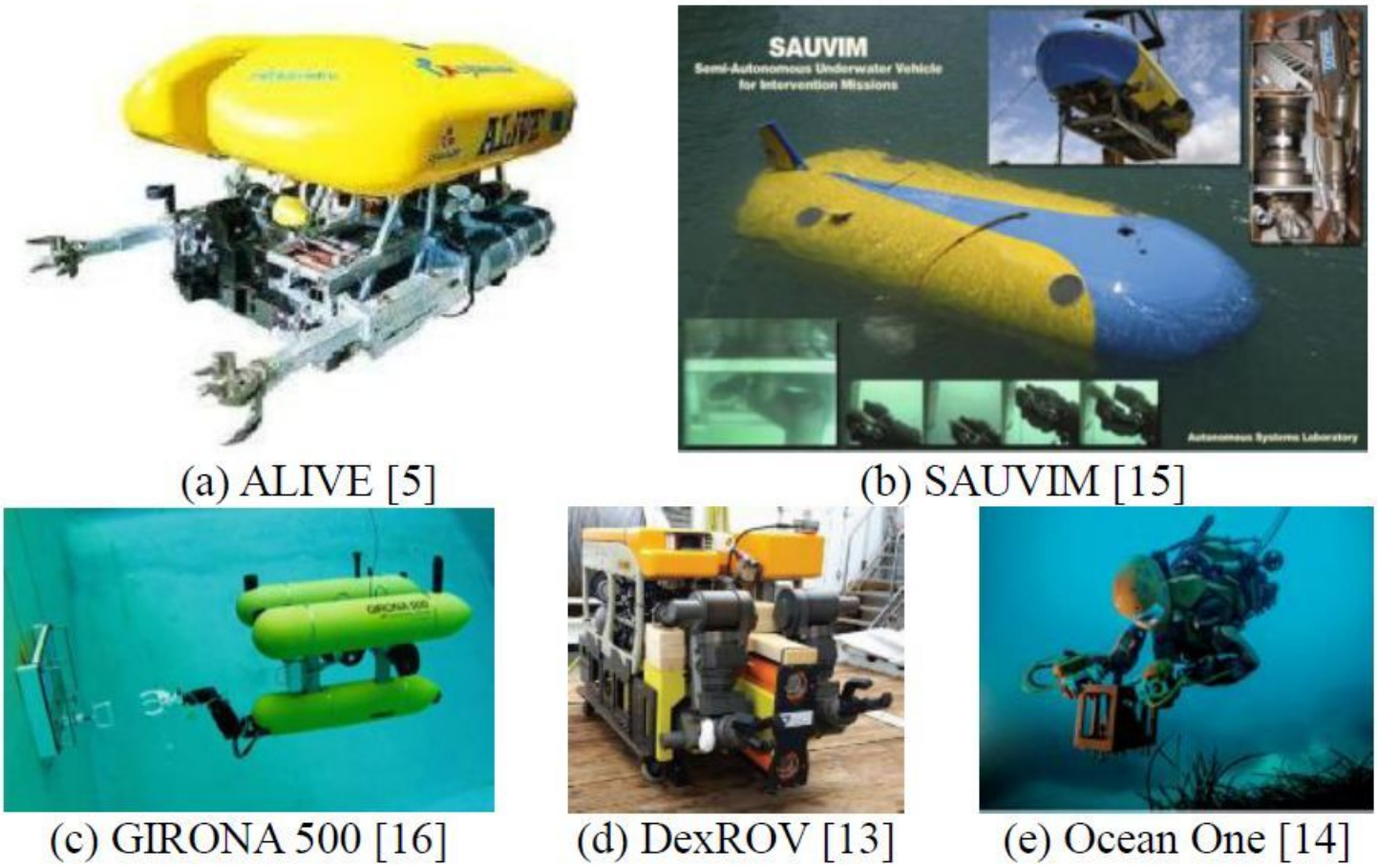

Figure 1

Different kinds of UVMS

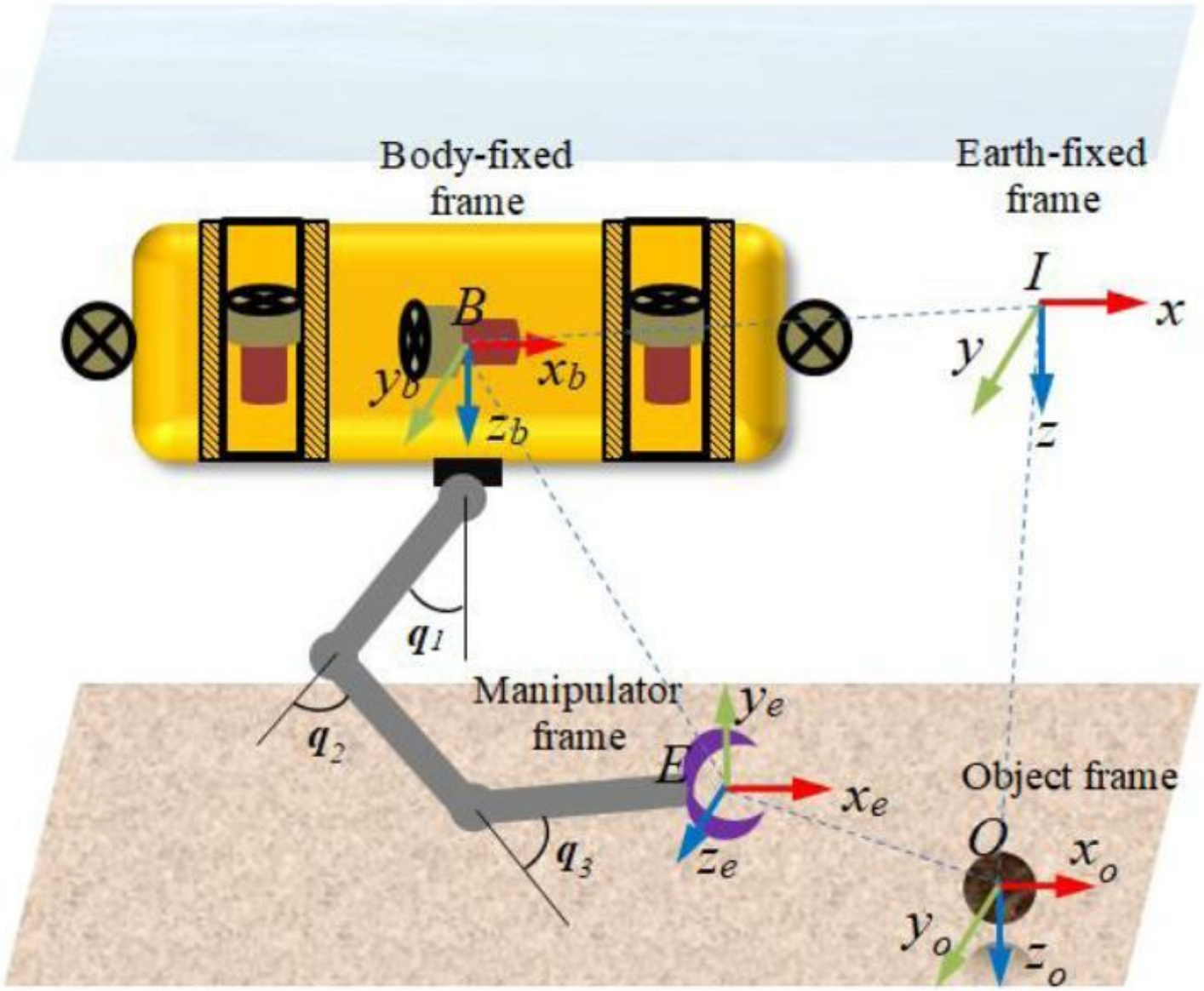

Figure 2

The model of UVMS equipped with a series manipulator and its coordinate frame

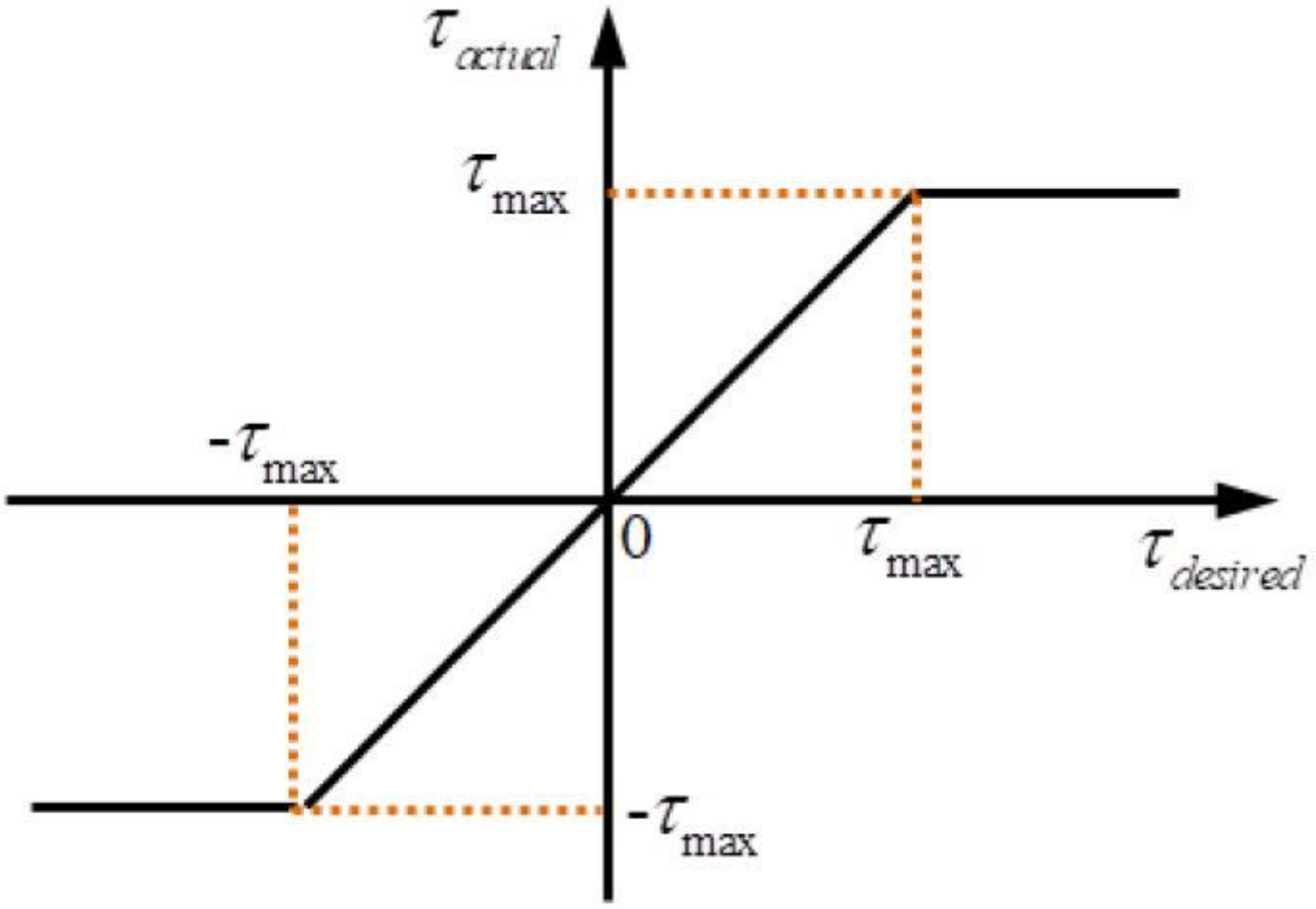

Figure 3

Desired input and actual output of actuator

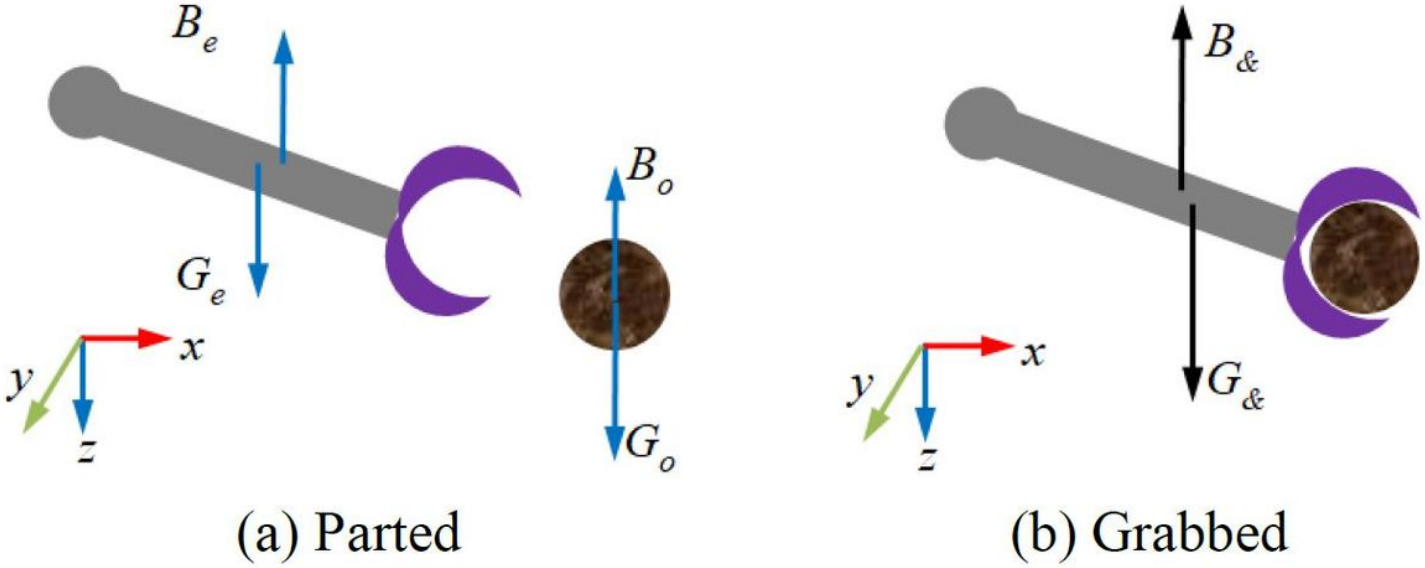

Figure 4

The process of grasping an object of end effector

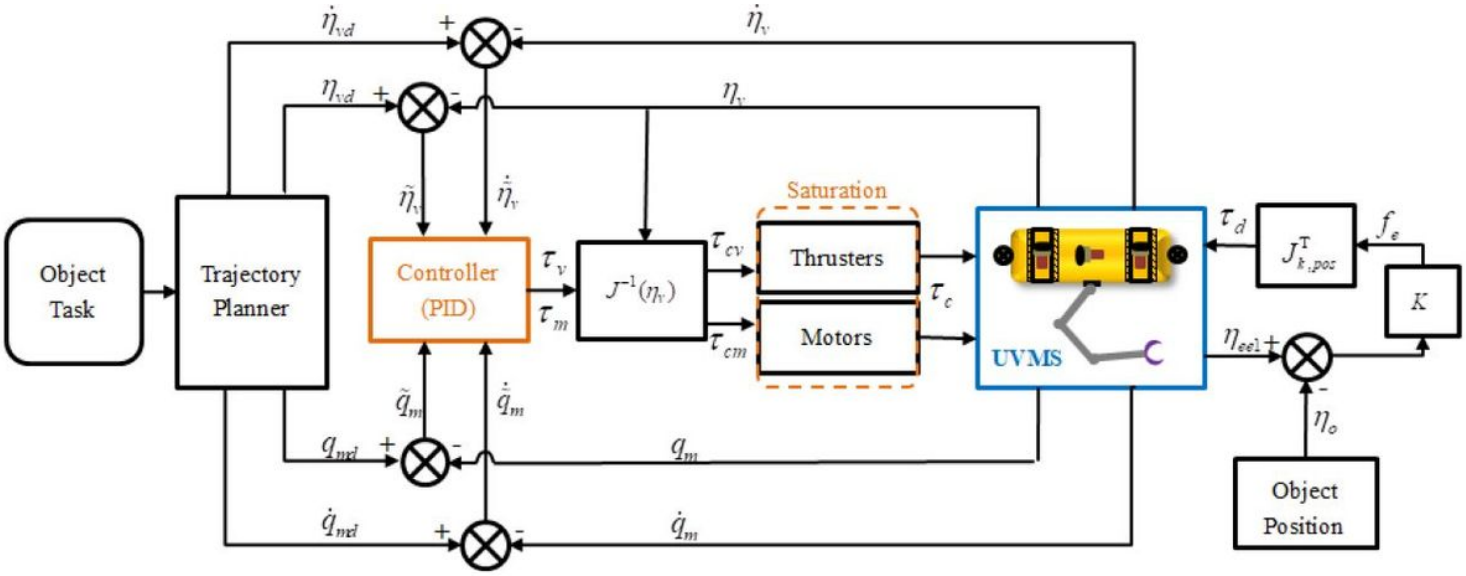

Figure 5

Schematic diagram of the UVMS control framework

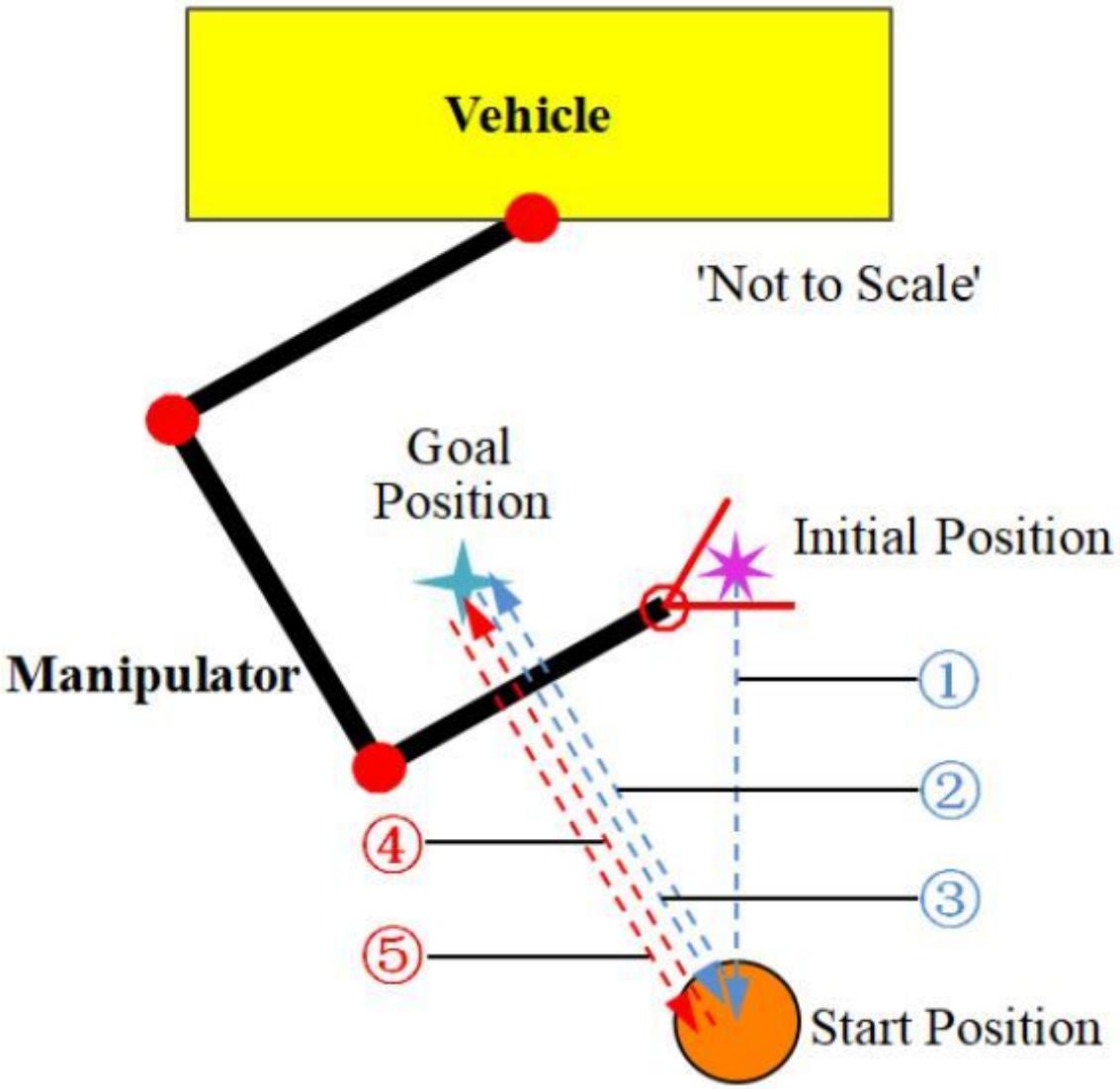

Figure 6

The process of grasping an object

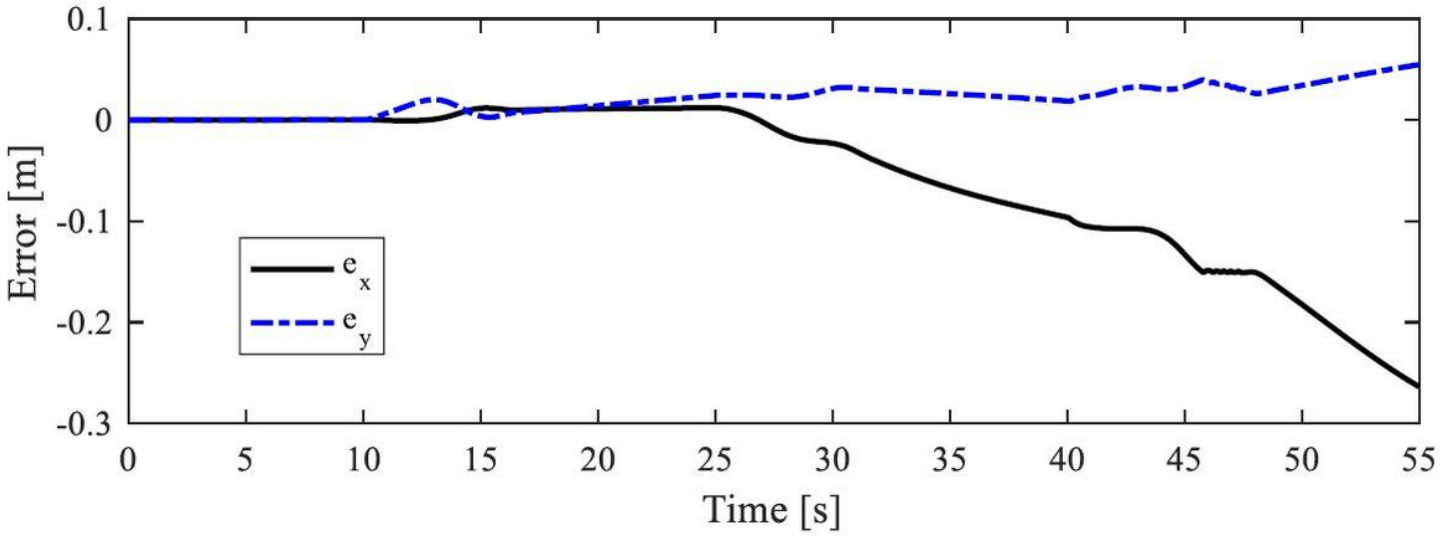

Figure 7

The position error of end effector without vehicle control

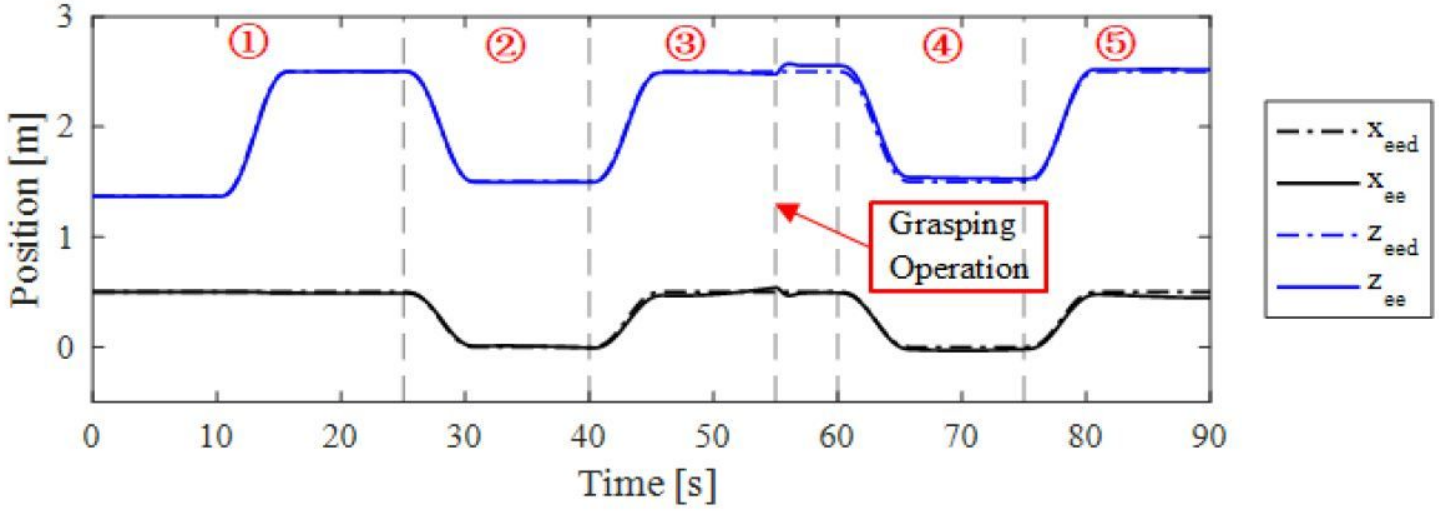

Figure 8

The desired and actual position of end effector with vehicle position control

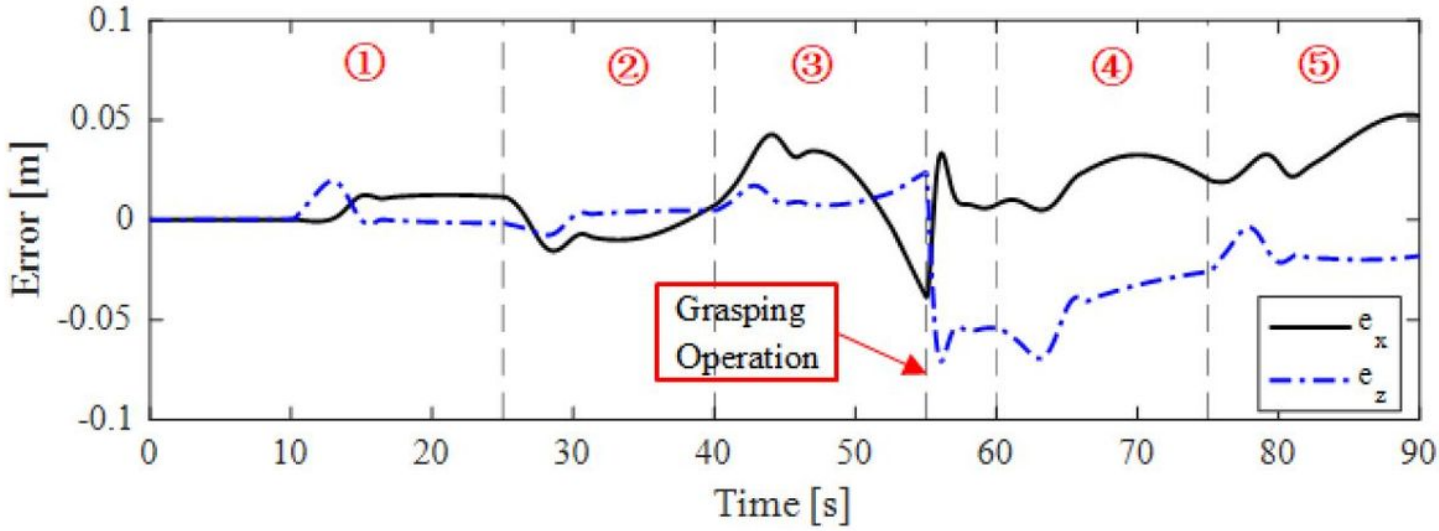

Figure 9

The position tracking error of end effector with vehicle position control

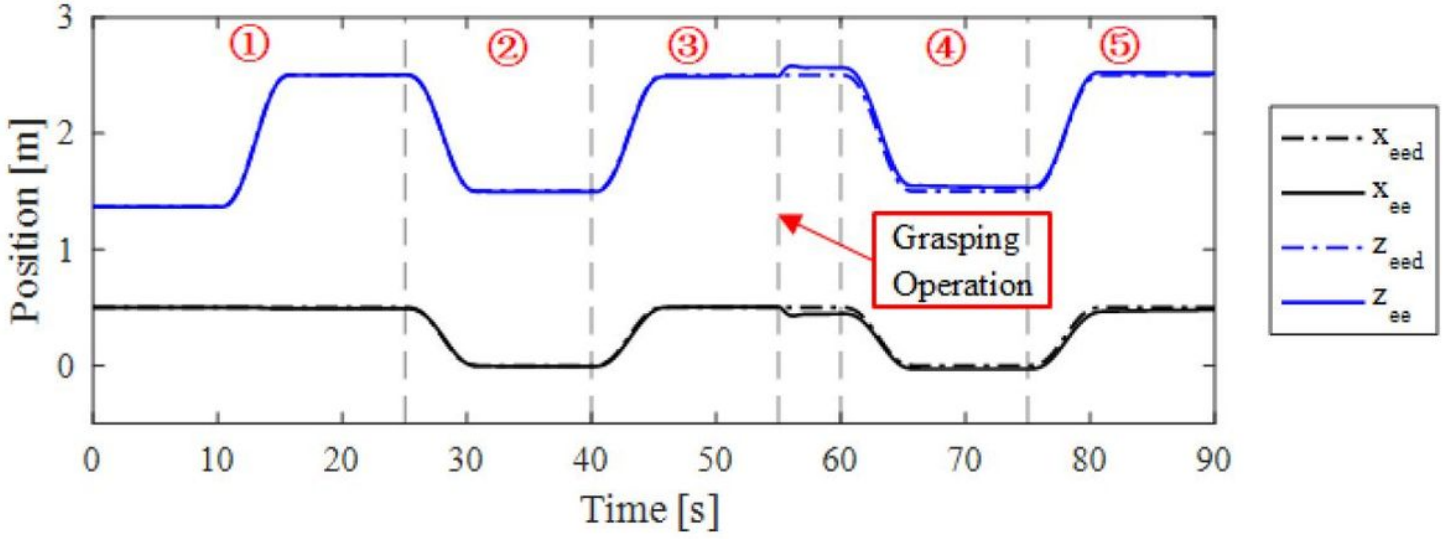

Figure 10

The desired and actual position of end effector with vehicle position and attitude control

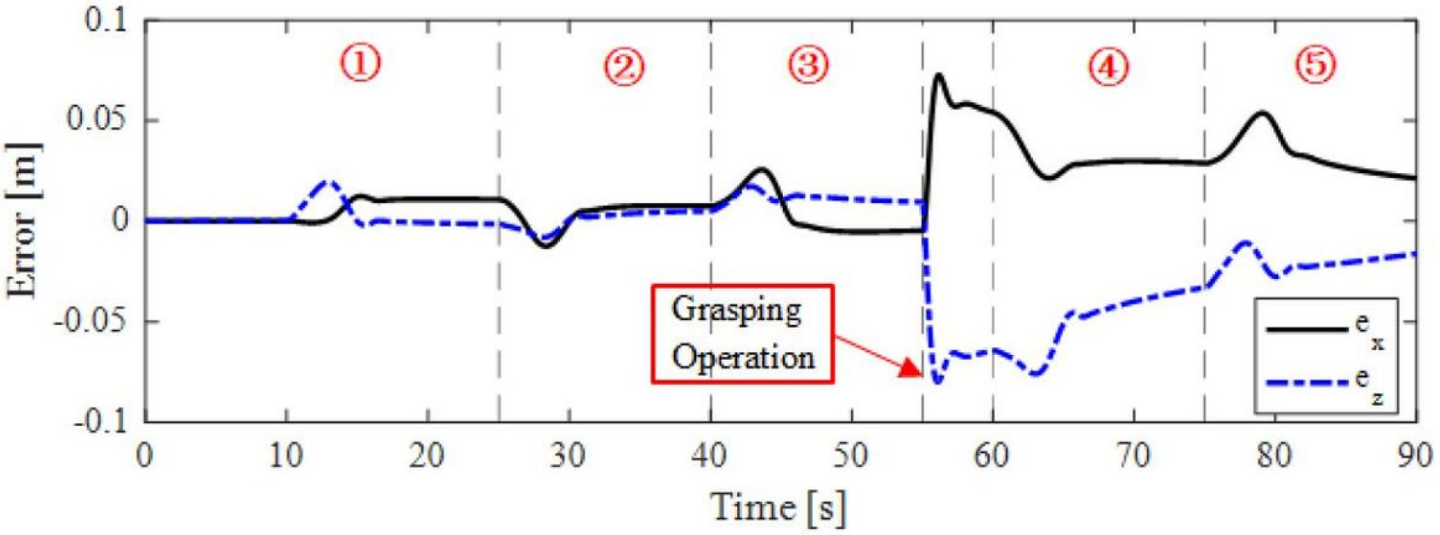

Figure 11

The position tracking error of end effector with vehicle position and attitude control

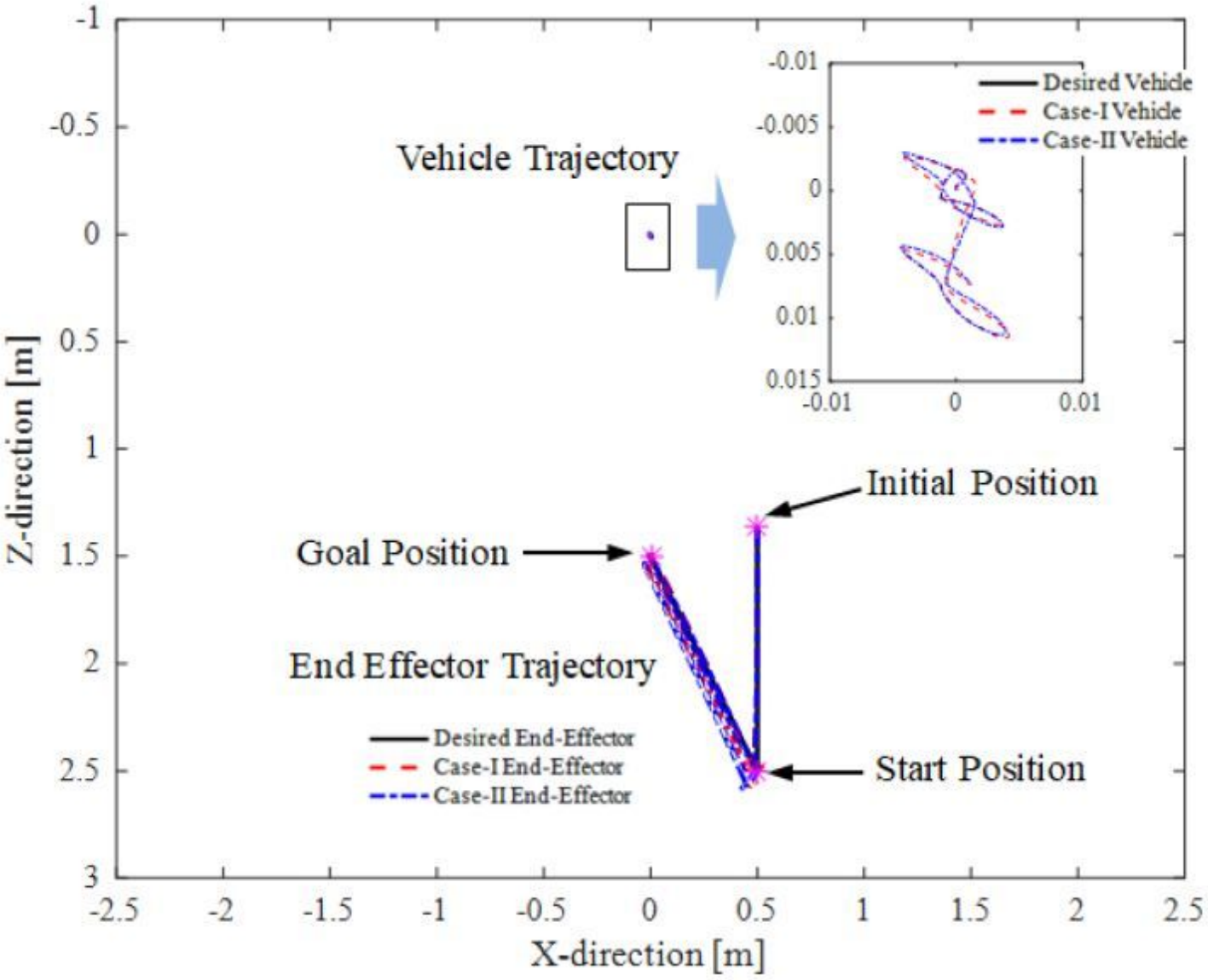

Figure 12

The trajectory of the position of the vehicle and the tip of end effector in vertical plane

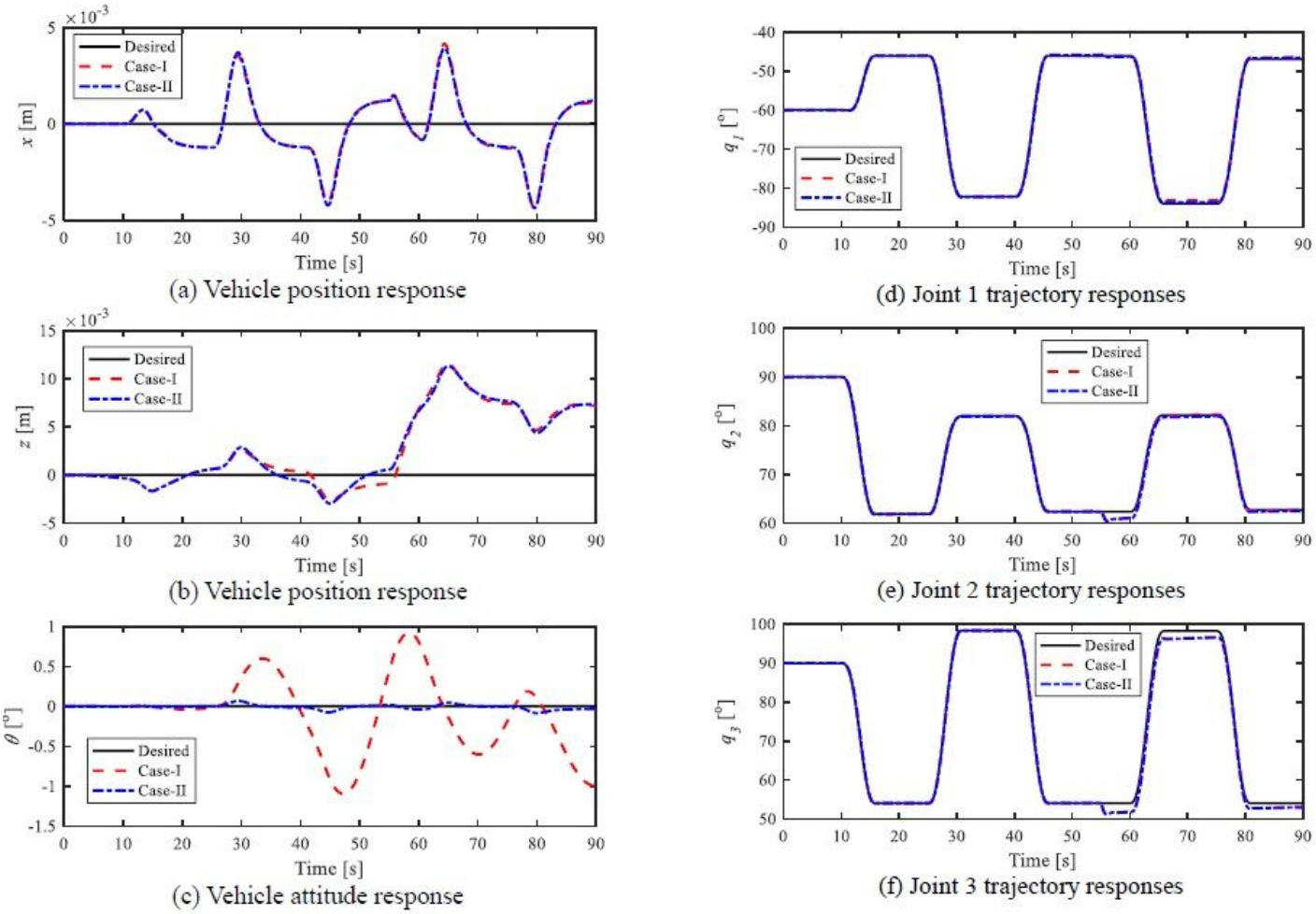

Figure 13

Vehicle and manipulator response

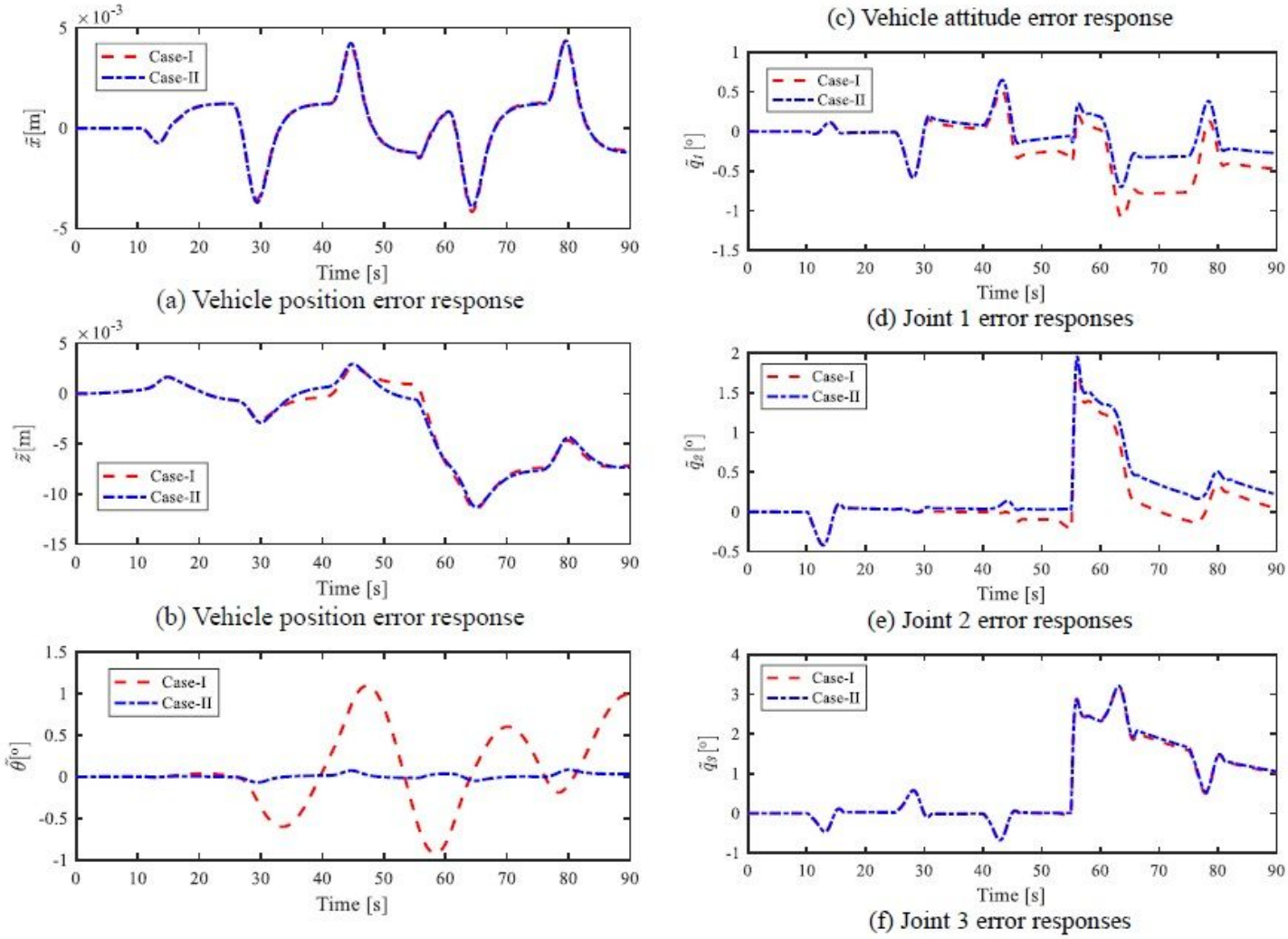

Figure 14

Vehicle and manipulator errors response

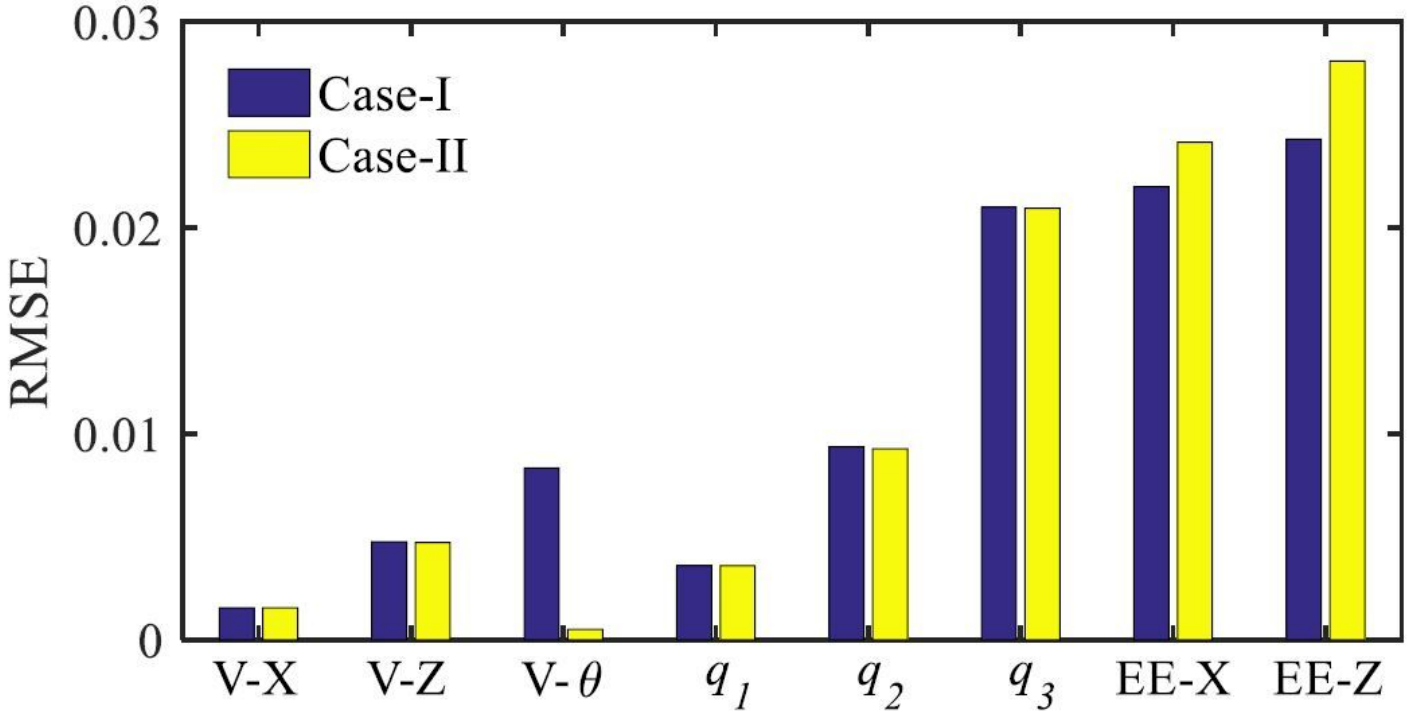

Figure 15

The RMSE of vehicle, manipulator and end effector